IEEE/CSC & ESAS EUROPEAN SUPERCONDUCTIVITY NEWS FORUM (ESNF), No. 10, October 2009.
Published in *AIP Conference Proceedings* **1219**, pp. 407-414 (2010)

THE PUZZLE OF TWO DIFFERENT SUB-MICROMETER TUNGSTEN-RICH DEPOSITS IN BULK YBCO: ONE ACTS AS PINNING CENTERS AND THE OTHER DOES NOT

Ravi-Persad Sawh, Roy Weinstein, Drew Parks, and Alberto Gandini

Beam Particle Dynamics Laboratory, Department of Physics, and Texas Center for Superconductivity, University of Houston
Houston, Texas, 77204, USA

ABSTRACT

Two types of large grain YBCO samples doped with tungsten oxide, one with platinum and the other without, were produced using a slow cooling process. Observations of the trapped magnetic flux density showed that the flux density of the W-doped, Pt-free samples did not change with W doping levels of up to 2.1 mol%. In contrast, the (W + Pt)-doped samples resulted in a monotonic improvement in trapped magnetic flux density as a function of W doping. Microstructure studies indicate that both types of samples contain profuse sub-micrometer deposits of a W-rich compound. The Pt-free samples contain $(W_{0.4}Y_{0.6})BaO_3$ deposits while the (W + Pt)-doped samples contain deposits of a $(W_{0.5}Pt_{0.5})YBa_2O_6$ compound. Both types of deposits are of essentially the same size and have comparable number density. The results are strikingly similar to an earlier experiment in which uranium doped, Pt-free, large grain YBCO also did not show any improvement in trapped magnetic flux density. The U-doped, Pt-free samples contain profuse sub-micrometer deposits of a $(U_{0.4}Y_{0.6})BaO_3$ compound, which have been shown to be ferromagnetic. The inability of both the $(W_{0.4}Y_{0.6})BaO_3$ and $(U_{0.4}Y_{0.6})BaO_3$ sub-micrometer deposits to act as pinning centers in self-field, suggest that this behavior is systematic.

KEYWORDS: Tungsten doping. Profuse sub-micrometer deposits. Ineffective pinning centers. Ferromagnetic non-pinning centers. Melt-textured YBCO high temperature superconductor.

INTRODUCTION

The introduction of pinning centers into high temperature superconductors (HTS) can dramatically increase critical current density (J_C), which is perhaps the most important property of HTS, apart from critical temperature (T_C). Pinning centers are small non-superconducting or poorly superconducting areas within the HTS that can trap magnetic fluxoids. Pinned magnetic fluxoids give rise to trapped magnetic flux density (B_{TRAP}). Bulk or melt-textured HTS with a high B_{TRAP} can be used in applications requiring large magnetic fields such as those involving motors and generators, or levitation.

Perhaps the most reasonable and inexpensive technique of introducing pinning centers into bulk HTS is by the method of chemical doping. In this method, chemical compounds are doped into the HTS powders and then melt-textured. One possible result is that the doped chemical compound interacts with the elements comprising the HTS during the texturing process to form profuse, small, non-superconducting deposits. These deposits then act as pinning centers and increase J_C. For example, when Y_2BaCuO_5 (Y211) is admixed into the $YBa_2Cu_3O_{7-\delta}$ (YBCO or Y123) powders and melt-textured, profuse deposits of Y211 remain after texturing. Y211 deposits have been shown to act as pinning centers and increase J_C in melt-textured YBCO [1]. Platinum (Pt) [2] or nanometer-size cerium oxide (nano-CeO_2) [3] doping into Y123 and Y211 powders, followed by melt-texturing, results in Y211 deposits that are reduced in size, and are also elongated in shape. This refinement of Y211 particles in YBCO also increases the number the number of pinning centers, resulting in an increase of J_C in bulk YBCO [3].

Two elements, both foreign to the HTS, have also been doped into HTS powders and successfully melt-textured [4]. During the melt-texturing process, the chemical compounds interact with elements from the HTS to form deposits. For example, when tungsten oxide (WO_3) and Pt are both added to Y123 and Y211 powders, and then textured, profuse deposits of $(W_{0.5}Pt_{0.5})YBa_2O_6$ (W–Pt–Y–Ba–O) were formed [5]. These W–Pt–Y–Ba–O deposits have been shown to act as effective uncorrelated point pinning centers and increase the self-field J_C of YBCO superconductor [5].

When WO_3 and an absence of Pt, or insufficient Pt are doped into Y123 and Y211 powders and melt-textured, the resulting deposits are *free* of Pt [5]. The Pt-free, W-rich deposits formed are as profuse as the W–Pt–Y–Ba–O deposits seen in (W + Pt)-doped YBCO superconductors. The pinning ability, chemical makeup and other important properties of the W–Y–Ba–O deposits and the W–Pt–Y–Ba–O deposits, are discussed in this report.

EXPERIMENTAL PROCEDURE

The tungsten dopant used in this experiment is in the form of WO_3. Metallic platinum (Pt) powder is another dopant. We also routinely use Y211 powder as a basic additive in melt-texturing YBCO samples. Y123 + 30 mol% Y211 powders were ball milled together with varying amounts of WO_3, with no added Pt. The WO_3 was varied from 0.0 mol% to 2.1 mol%. The 0.0 mol% WO_3 samples were controls in the W-doped, Pt-free, experiment. For comparison to (W + Pt)-doped samples, we used 4.1 or 5.2 mol% Pt as the dopant in the Y123 + 30 mol% Y211 + varying amounts of WO_3 powders. Here again, WO_3 was varied from 0.0 mol% to 2.1 mol%. The control samples for the (W + Pt)-doped experiment were those containing 0.0 mol% WO_3.

The ball-milled powders were pressed into cylindrical samples 1.9 cm in diameter, top-seeded with $SmBa_2Cu_3O_{7-\delta}$ (Sm123), and melt-textured using a slow cooling process [6]. Textured samples were subsequently annealed in flowing oxygen gas. The resulting cylindrical samples were 1.5 cm diameter and 0.6 cm thickness, and were single grains as shown by trapped magnetic flux density (B_{TRAP}) studies. At least 4 single grain samples were produced for each combination of dopants at each level of doping.

Trapped magnetic flux density (B_{TRAP}) was measured on all samples. In order to measure B_{TRAP}, samples were cooled in liquid nitrogen while in the field of a 0.8 T electromagnet with the c-axis of the sample parallel to the applied field. B_{TRAP} was measured with an axial direction hall sensor, 0.6 mm away from the surface of the sample. (B_{TRAP} represents the maximum trapped magnetic flux density of samples after the activating field was removed). It is well established that J_C can be obtained from B_{TRAP} and a geometrical function of both the diameter and thickness of single grains [7]. The drawback of this method of measuring J_C is that J_C can only be found in the self-field, i.e., $B_{APPLIED} = B_{TRAP}$.

Critical temperature (T_C) was measured on cylindrical samples, 1.5 cm diameter x 0.15 cm thick cut from larger melt-textured single grain samples. An APD Cryogenics Helium Refrigerator in an applied field of 6 mT was used to measure T_C.

Sample microstructure was studied with the aid of a JEOL JXA-8600 electron microprobe. Elemental analysis was done using the wavelength dispersive X-ray spectrometer (WDX) and the energy dispersive X-ray spectrometer (EDX) attachments of the electron microprobe.

RESULTS AND DISCUSSION

Trapped Magnetic Flux Density and Self-Field J_C

The most telling result of this experiment is the B_{TRAP} of the W-doped, Pt-free, samples compared to the B_{TRAP} of the (W + Pt)-doped samples. The results are summarized in FIGURE 1. FIGURE 1 is a graph of the enhancement (R_M) of B_{TRAP} versus mol% doping of WO_3, where $R_M \equiv B_{TRAP}$(mol% WO_3 + mol% Pt)/B_{TRAP}(0.0 mol% WO_3 + mol% Pt). As shown in FIGURE 1, for the W-doped, Pt-free samples, self-field J_C is essentially unchanged for all WO_3 doping levels used in this experiment. This is an unexpected result. On the other hand, for the (W + Pt)-doped samples, R_M increases monotonically and reaches a maximum of ~ 1.4 for samples containing 1.7 mol% WO_3 and 5.2 mol% Pt (see FIGURE 1). R_M then decreases for samples doped with more than 1.7 mol% WO_3 and 5.2 mol% Pt. A maximum R_M of 1.4, for the (W + Pt)-doped samples, corresponds to a 40% increase in J_C as observed in a self-field that is also 40% higher. These results indicate a puzzle: in samples where Pt is *not* doped into the WO_3 + Y123 + Y211 powders, the result is the formation of *ineffective* pinning centers; however, the addition of Pt into the same chemical mixture results in the creation of *effective* pinning centers.

We defined R_M as the enhancement of B_{TRAP}. For the W-doped, Pt-free samples, R_M is defined as the ratio of B_{TRAP} of samples doped with WO_3, to samples with 0.0 mol% WO_3 (controls). For the (W + Pt)-doped samples, R_M is the ratio of B_{TRAP} of the (W + Pt)-doped samples to the samples doped with Pt alone. Therefore, R_M compares the B_{TRAP} of W-doped samples to the appropriate Pt-doped or Pt-free control samples. By presenting results as the ratio R_M, we normalize out the effects of other pinning centers, thereby focusing only on the effect of the combination of WO_3 and Pt (or no Pt) doping.

For W-doped, Pt-free samples, the average B_{TRAP} of 4 cylindrical samples, 1.5 cm in diameter x 0.6 cm thick, is ~ 225 mT at all WO_3 doping levels investigated in this experiment. A B_{TRAP} of ~ 225 mT corresponds to a self-field J_C of ~ 8,000 A-cm^2. A self-field J_C of ~ 8,000 A-cm^2 is indicative of good quality, melt-textured YBCO samples produced with only Y123 and Y211 [7]. For (W + Pt)-doped samples, B_{TRAP} increases

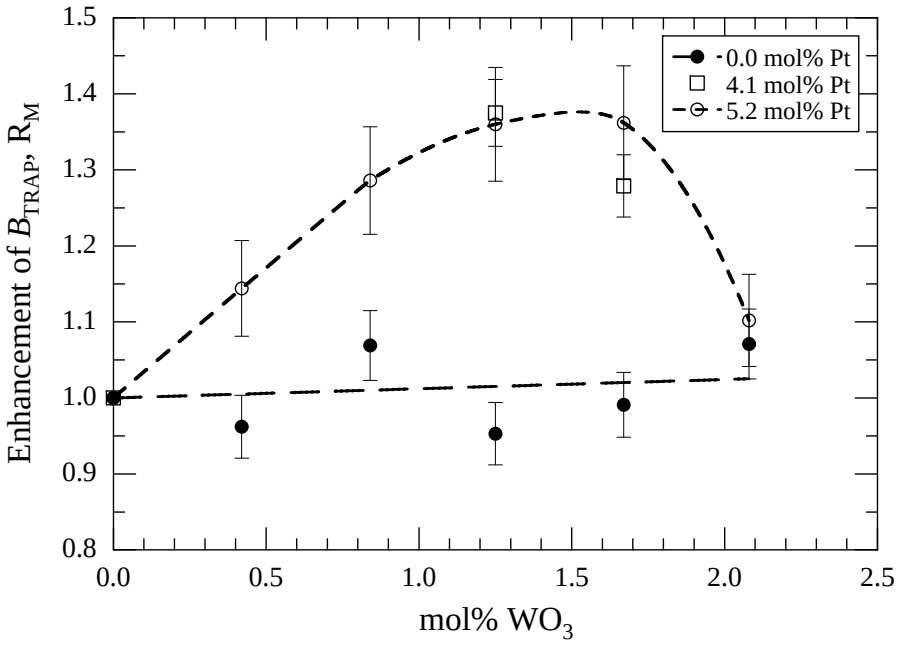

FIGURE 1. Graph of the enhancement (R_M) of B_{TRAP} as a function of mol% WO_3 doped into YBCO for three different Pt doping levels. $R_M \equiv B_{TRAP}$(mol% WO_3 + mol% Pt)/B_{TRAP}(0.0 mol% WO_3 + mol% Pt). Each point represents the average of measurements of four cylindrical samples, 1.5 cm in diameter x 0.6 cm thick. Dashed lines are drawn to guide the eye.

from ~ 275 mT (self-field J_C ~ 9,700 A-cm^2), for control samples containing 5.2 mol% Pt and 0.0 mol% WO_3, to a maximum of ~ 375 mT (self-field J_C of ~ 13,250 A-cm^2), for samples doped with ~ 1.7 mol% WO_3 and 5.2 mol% Pt. The higher initial value of B_{TRAP} is due to the refinement of Y211 particles by Pt. Even though good quality single grains are produced at any WO_3 doping level, for both Pt-doped and Pt-free samples, it is a paradox that B_{TRAP} *neither increases nor decreases* for all W-doped, Pt-free samples produced in this experiment.

The unchanging behavior of R_M as a function of mol% WO_3 suggests that non-pinning, or very ineffective pinning centers are formed in W-doped, Pt-free samples compared to (W + Pt)-doped samples.

Microstructure

Electron microprobe images are shown in FIGURE 2 for samples doped with WO_3, both with and without Pt doping. For the W-doped, Pt-free sample, profuse deposits of a W–Y–Ba–O compound are seen (small bright spots in the left side image of FIGURE 2). The qualitative composition of the W-rich particles was determined from energy dispersive X-ray (EDX) data. The deposits appear to be uniformly distributed in the YBCO. The deposits are almost spherical in shape with an average diameter determined to be less than 500 nm. Their observed diameter

does not appear to change with WO_3 doping level, instead the number of deposits increase as the doping level of WO_3 increases. Analysis of the Y123 background with EDX and wavelength dispersive X-ray data (WDX), indicate that there is no substitution of W into the YBCO crystal structure. As a result, no change in critical temperature (T_C) is expected.

Similarly, for the (W + Pt)-doped samples, there are also profuse deposits (see right side image of FIGURE 2) of a W–Pt–Y–Ba–O compound as identified from analysis of the EDX data. They are also quasi-spherical in shape, and are well distributed. Their size

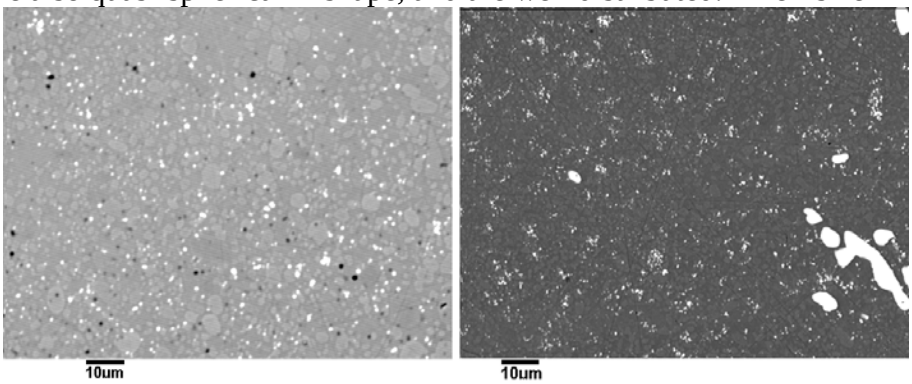

FIGURE 2. Electron microprobe images of textured YBCO superconductors. The sample on the left is Y123 + 30 mol% Y211 + 0.84 mol% WO_3. Profuse W-rich deposits are the small bright white spots. Y211 particles (pale gray in color) are embedded in a gray Y123 background. The sample on the right is Y123 + 30 mol% Y211 + 4.12 mol% Pt + 1.25 mol% WO_3. (W + Pt)-rich deposits are profuse small bright white spots while Y211 deposits appear as pale black in color and the YBCO background is black in color.

appears to average ~ 400 nm in diameter, about the same size as the W–Y–Ba–O particles seen in W-doped, Pt-free YBCO samples. As with the W-doped, Pt-free samples, the size of the deposit do not appear to change with W-doping levels, instead the number of deposits increases with increasing W-doping levels. They are also comparable in number density to the W–Y–Ba–O deposits. Again, there is no substitution of either W or Pt into the YBCO matrix as indicated by WDX and EDX analyses.

To determine the composition of the W–Y–Ba–O deposits in W-doped, Pt-free samples, and W–Pt–Y–Ba–O particles seen in (W + Pt)-doped YBCO, an analysis of WDX data was performed. This analysis is shown in FIGURE 3. The electron beam of the microprobe measures the composition of an area on the image. A typical W–Y–Ba–O or W–Pt–Y–Ba–O deposit within that area is smaller than the size of the electron beam, as a

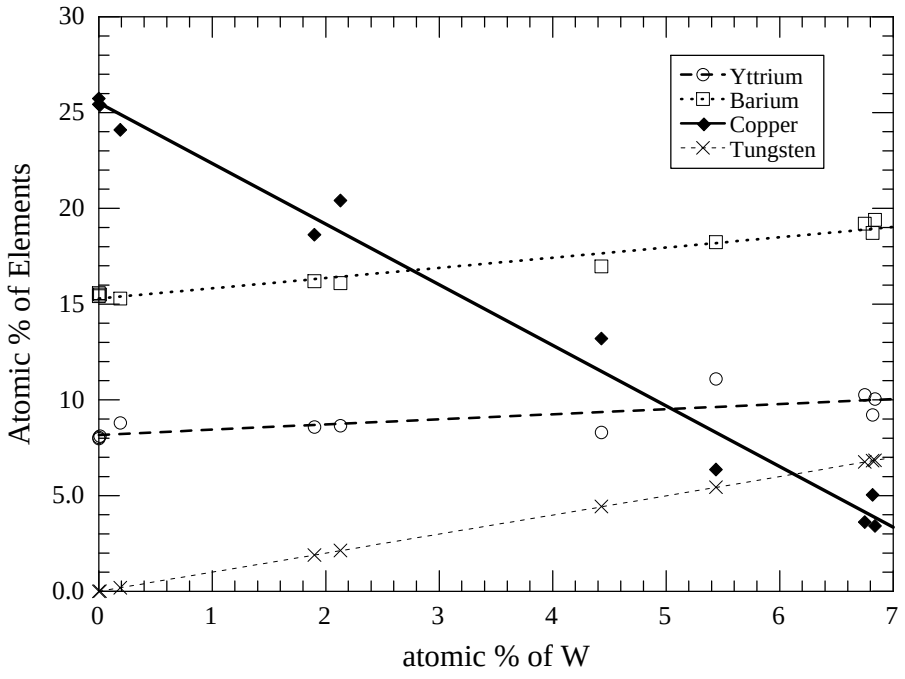

FIGURE 3. Graph of atomic % of all elements contained in W-doped, Pt-free YBCO samples versus atomic % of W. Data is taken from the WDX analysis of various bright spots of W–Y–Ba–O particles, which vary somewhat in size. The lines represent the best rms straight line fit to the data.

result, information on both the background Y123 and the W-rich deposit, is recorded.
Using the observation that W does not substitute into the YBCO crystal matrix; we can determine the composition of the W-rich particles, which vary somewhat in size, by subtracting the background Y123. From the analysis shown in FIGURE 3, we determined the composition of the W-rich phase in W-doped, Pt-free samples to be $(W_{0.4}Y_{0.6})BaO_3$ (W–Y–Ba–O). A similar analysis (not shown) of the (W + Pt)-doped samples showed that the W-rich phase is $(W_{0.5}Pt_{0.5})YBa_2O_6$ (W–Pt–Y–Ba–O), which confirmed the results of an earlier experiment [5]. The W–Y–Ba–O is single perovskite in structure while the W–Pt–Y–Ba–O compound has a double perovskite structure. Perhaps it is the difference in chemical composition and crystal structure that is responsible for the inability of the W–Y–Ba–O to act as effective pinning centers, compared to the W–Pt–Y–Ba–O deposits which are effective uncorrelated point pinning centers.

It is worth pointing out that in determining the composition of the deposits of the W-doped, Pt-free samples, we also concluded that copper (Cu) is *not* a component of the W–Y–Ba–O compound. This is easily seen in FIGURE 3 where all the elements increase in atomic % with increasing size, or increasing W atomic % *except* Cu, which instead decreases. A similar analysis (not shown) of the (W +Pt)-doped samples also concluded that Cu is not a component of the W–Pt–Y–Ba–O particles.

Critical Temperature (T_C)

As previously noted, for both the W-doped, Pt-free and the (W + Pt)-doped samples, we did not observe any substitution of either W or Pt into the YBCO crystal matrix. Therefore, we do

not expect any significant change in critical temperature (T_C). T_C measurements are shown in FIGURE 4. The method of measuring T_C was described in the experimental section. It should be noted that the samples used to measure T_C were cut from the larger single grains and were cylindrical in shape with a diameter of 1.5 cm and a thickness of 0.15 cm. T_C is defined as the midpoint of the temperature transition. In all samples measured, the T_C is determined to be between 90 K and 91 K. The estimated error in our T_C measurement is ± 0.5 K. With the samples being large, the value obtained for T_C

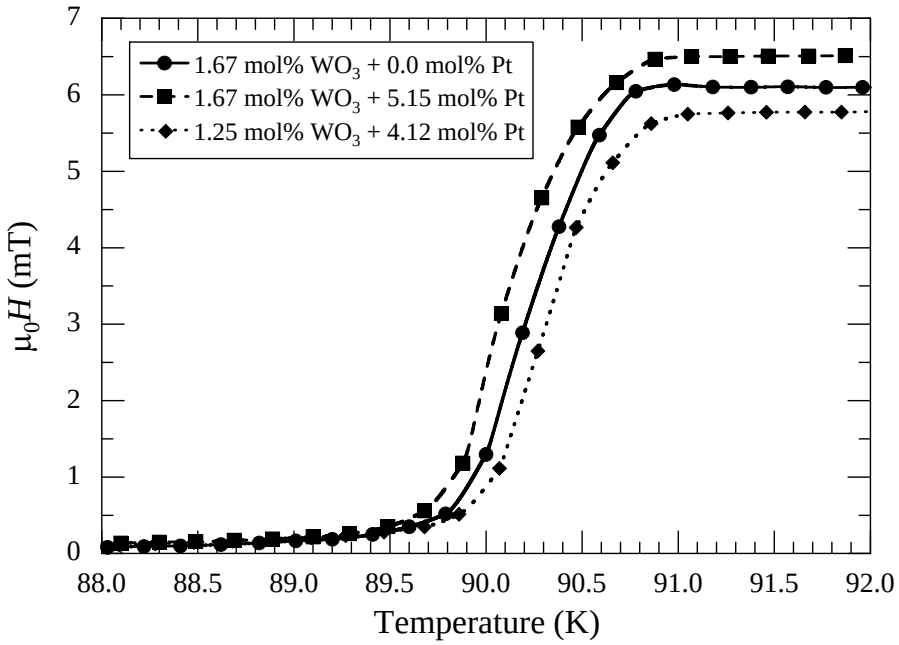

FIGURE 4. Critical temperature measurements of selected YBCO samples used in this experiment.

is rather typical for bulk YBCO superconductors [8-9]. The T_C transition of all samples appears to be sharp. Therefore, changes in T_C are not the reason for the W–Y–Ba–O deposits being very ineffective pinning centers when compared to W–Pt–Y–Ba–O deposits. Since T_C is not changed significantly for all samples measured, the inability of the W–Y–Ba–O compound to act as effective pinning centers is still a puzzle.

An Earlier Experiment with Uranium-Doped, Pt-Free Samples

In an earlier study of uranium-doped, Pt-free YBCO, similar surprising results of B_{TRAP} were found [8]. U-doped, Pt-free melt-textured YBCO samples contained profuse sub-micrometer sized deposits of a U–Y–Ba–O compound. In measurements of B_{TRAP}, there was neither an increase nor decrease as mol% U was varied, just as in the W-doped, Pt-free samples of the present experiment. Just like the W–Y–Ba–O deposits, B_{TRAP} measurements indicate that the U-rich deposits, identified as $(U_{0.4}Y_{0.6})BaO_3$ (U–Y–Ba–O), are also ineffective pinning centers, and do not increase the self-field J_C of samples. These results were compared to (U + Pt)-doped samples that contained profuse sub-micrometer deposits of a $(U_{0.6}Pt_{0.4})YBa_2O_3$ (U–Pt–Y–Ba–O) compound [9]. The U–Pt–Y–Ba–O deposits are effective pinning centers and increase

B_{TRAP} in the same manner as the W–Pt–Y–Ba–O deposits, i.e., we observed a monotonic increase in B_{TRAP} as U doping levels were increased. Therefore the puzzle of non-pinning deposits is not limited to tungsten, it is more systematic.

To further investigate the properties of the U–Y–Ba–O compound, we produced the U–Y–Ba–O compound outside YBCO. The compound was produced by a solid-state reaction of peroxides, oxides or carbonates of the elements comprising the U–Y–Ba–O compound. After repeated grinding and heat treatment, the magnetic moment of small samples of the compound were measured on a vibrating sample magnetometer (VSM).

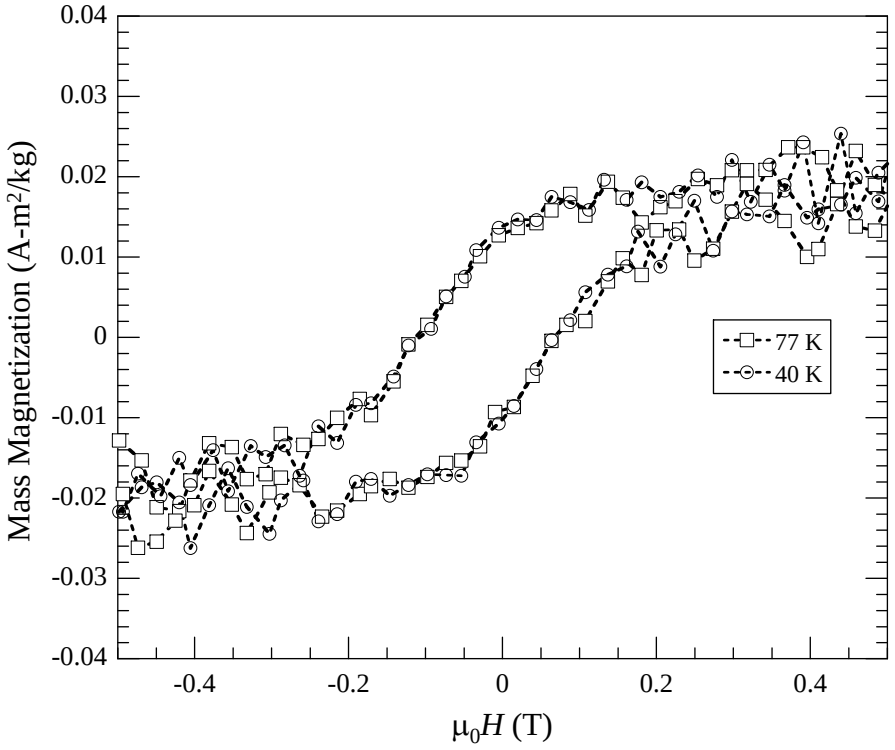

FIGURE 5. Mass magnetization measurements at two different temperatures for the U–Y–Ba–O compound produced outside YBCO by a solid-state reaction of compounds of the constituent elements.

The chemical makeup of the U–Y–Ba–O compound produced outside YBCO was confirmed to be the same as that inside U-doped, Pt-free YBCO by X-ray diffraction studies (these results will be published elsewhere). Some results of the VSM studies of the externally produced U–Y–Ba–O compound are shown in FIGURE 5. At temperatures up to 294 K, the behavior of mass magnetization versus applied magnetic field strength indicates that the U–Y–Ba–O compound is a ferromagnetic material. A similar experiment done on the U–Pt–Y–Ba–O compound indicates that the behavior is that of a typical paramagnet. Additionally, we speculate that the W–Y–Ba–O compound may also be ferromagnetic since its chemical composition and crystal structure is identical to U–Y–Ba–O, except with W replacing U. The ferromagnetic behavior of U–Y–Ba–O and the probable ferromagnetic nature of W–Y–Ba–O, suggest that this may be a possible reason as to why the single perovskite compounds are non-pinning, or ineffective pinning centers in the self-field region when compared to paramagnetic double perovskite deposits.

CONCLUSION

The experiments described in this paper suggest that in high temperature superconductors, there probably exists a class of sub-micrometer ferromagnetic deposits, with a single perovskite structure, that are non-pinning, or are ineffective pinning centers in the self-field region. In particular, we have shown that profuse sub-micrometer deposits of $(W_{0.4}Y_{0.6})BaO_3$ are ineffective pinning centers when compared to $(W_{0.5}Pt_{0.5})YBa_2O_6$ deposits. In earlier experiments we have also shown that deposits of $(U_{0.4}Y_{0.6})BaO_3$ are ineffective pinning centers when compared to $(U_{0.6}Pt_{0.4})YBa_2O_6$ deposits. We have also shown that the compound $(U_{0.4}Y_{0.6})BaO_3$ is ferromagnetic, and it is perhaps this property that limits the pinning ability of this family of compounds in the self-field region.

ACKNOWLEDGEMENTS

We thank the staff of the Materials Characterization Facility at the Texas Center for Superconductivity at the University of Houston (TCSUH) for their support in the microprobe studies. This work was supported by grants from the U.S. Army Research Office, the Welch Foundation under Grant E-1380, and the State of Texas via TCSUH.

REFERENCES

1. Murakami, M., Yamaguchi, K., Fujimoto, H., Taguchi, T., Koshizuka, N. and Tanaka, S. *Cryogenics* **32**, pp. 930-935 (1992).
2. Ogawa, N., Hirabayashi, I. and Tanaka, S. *Physica C* **177**, pp. 101-105 (1991).
3. Sawh, R. –P., Weinstein, R., Parks, D. and Obot, V. *IEEE Trans. Appl. Supercond.* in press.
4. Weinstein, R. and Sawh, R. –P. *Physica C* **383**, pp. 438-444 (2003).
5. Sawh, R. –P., Weinstein, R., Parks, D., Gandini, A., Ren, Y. and Rusakova, I. *Physica C* **383**, pp. 411-416 (2003).
6. Salama, K., Selvamanickam, V. and Sun, K. *Appl. Phys. Lett.* **54**, pp. 2352-2354 (1989).
7. Chen, I. –G., Liu, J., Weinstein, R. and Lau, K. *J. Appl. Phys.* **72**, pp. 1013-1020 (1992).
8. Sawh, R. –P., Weinstein, R., Parks, D., Obot, V. and Gandini, A. *IEEE Trans. Appl. Supercond.* **17**, pp. 3705-3708 (2007).
9. Sawh, R. –P., Ren, Y., Weinstein, R., Hennig, W. and Nemoto, T. *Physica C* **305**, pp. 159-166 (1998).